

Electronic Supplementary Information (ESI)

Nanocrystals Colloidal deposition process: An advanced method to prepare high performance hematite photoanodes for water splitting

Ricardo H. Gonçalves and Edson R. Leite*

Department of Chemistry, Federal University of So Carlos, 13565-905, Sao Carlos, SP, Brazil

Experimental Procedure

Materials. Iron acetylacetonate (III) (99.99%), tin (IV) tert-butoxide, oleyl alcohol and oleic acid were purchased from Aldrich Chemical Co and FTO/aluminum borosilicate was purchased from Solaronix S.A.

Magnetite/maghemite nanocrystals. Magnetite (Fe_3O_4) was synthesized using the method described in reference [1]. In this synthesis, 12 g of iron (III) acetylacetonate were solubilized in 100 ml of oleyl alcohol. This solution was heated to 260 °C for 1 h in a nitrogen atmosphere. After this reaction time, the colloid which formed was cooled and separated with the addition of 300 ml of acetone and the assistance of an external magnetic field. The separated nanocrystals were re-dispersed in 20 mL of toluene and centrifuged at 14,000 rpm for 5 min to remove nanocrystal agglomerates. The magnetite nanocrystals were transformed to maghemite ($\gamma\text{-Fe}_2\text{O}_3$) to avoid Fe^{2+} ; oxygen gas was bubbled into the magnetite colloid at 120 °C for 2 h. This transformation can be identified by the brownish color of the colloid. Finally, the nanocrystal concentration was adjusted to 190 mg.mL^{-1} .

Tin doping precursor. Initially, a tin stock solution was prepared with the addition of 1 mmol of tin (IV) tert-butoxide in 1:1 ml of toluene/oleic acid. The oleic acid was used to stabilize the organometallic precursor in toluene and to protect against hydrolyzation.

Thin film preparation. Prior to the deposition, the FTO substrate (typical size 2 cm x 1 cm) was washed with an HCl/HNO₃ solution for 30 min and rinsed several times with pure water. Then the same substrate was immersed in a sodium hydroxide solution for 30 min and again rinsed with pure water; finally, the substrate was dried at 110°C for 2 hours. The colloidal nanocrystal deposition was carried out by a magnetic field-assisted dip coating process. First, a container was fitted with two N50 grade (1.4T) NdFeB magnets (see Scheme 1 and Figure S1 for details regarding this container). For undoped hematite, 2 mL of concentrated stock dispersion (190 mg.mL⁻¹) of maghemite colloid was added between these magnets, and the dip coating process was completed with an insertion speed of 60 mm/min and withdrawal speed of 80 mm/min. (see dip coating process detail in the Figure S1c). Under optimized conditions, the nanocrystalline thin film was rapidly inserted into a furnace tube at 850 °C and quickly removed after 20 min. The doped hematite thin film was produced with colloidal maghemite nanocrystals, which were adjusted in the same concentration (190 mg.mL⁻¹), and a mass of 8% tin (IV) tert-butoxide was added. The doped thin film was inserted into a furnace at 850 °C and removed directly to room temperature after 3 min of heat treatment.

Photoelectrochemical characterization. Photoelectrochemistry measurements were conducted in a standard three-electrode cell by using: 1) the hematite film as the working electrode (the working surface area was 0.19 cm²); 2) Ag/AgCl in a KCl saturated solution as the reference electrode; and 3) the platinum plate as a counter electrode. A 1.0 M NaOH solution (Aldrich, 99.99%) in highly pure water (pH=13.6, 25 °C) was used as the electrolyte. A scanning potentiostat (Potentiostat/Galvanostat μ Autolab III) was used to measure the dark and illuminated currents at a scan rate of 20 mV/s. Sunlight (100 mW/cm²) was simulated with a 250 W Xenon lamp (Osram, ozone free) and AM1.5 filter (Newport Corp.). The incident photo-to-current conversion efficiency (IPCE) was measured as a function of the excitation wavelength (λ) using a 300 xenon lamp coupled monochromator (QE/IPCE measurement) (KIT Newport Corp.). The IPCE plot was calculated by considering the following the equation of reference^[12]. The electrochemical impedance spectroscopy (EIS) measurement was taken in a NaOH solution under dark

conditions using a Metrohm autolab Model PGSTA T204. The Nyquist plot was constructed from 1.75 V_{RHE} to 0.8 V_{RHE} for both doped and undoped hematite; the Mott-Schottky plot was extracted in the linear region at 1 KHz. For the Mott-Schottky analysis, the geometric area was corrected by multiplying its value by a roughness factor which was estimated by an atomic force microscopy (AFM) measurement. Roughness factors used for undoped and Sn-doped hematite films were 15.6 and 6.2, respectively. For the roughness factor calculation, the film and hematite single crystal roughness measured by AFM (roughness factor = film hematite roughness/hematite single crystal roughness) was considered.

Transmission Electron Microscopy (TEM) Characterization. The TECNAI F20 FEI microscope was used to obtain high-resolution transmission electron microscopy (HRTEM) and scanning transmission electron microscopy (STEM) with dispersive X-rays analysis (STEM/EDX) operating at 200 kV. The *in situ* TEM experiment was conducted in a temperature range from 25 to 850 °C at rate of 50 °C/min⁻¹. Videos were recorded at 5 frames /seconds and a resolution of 720 x 480.

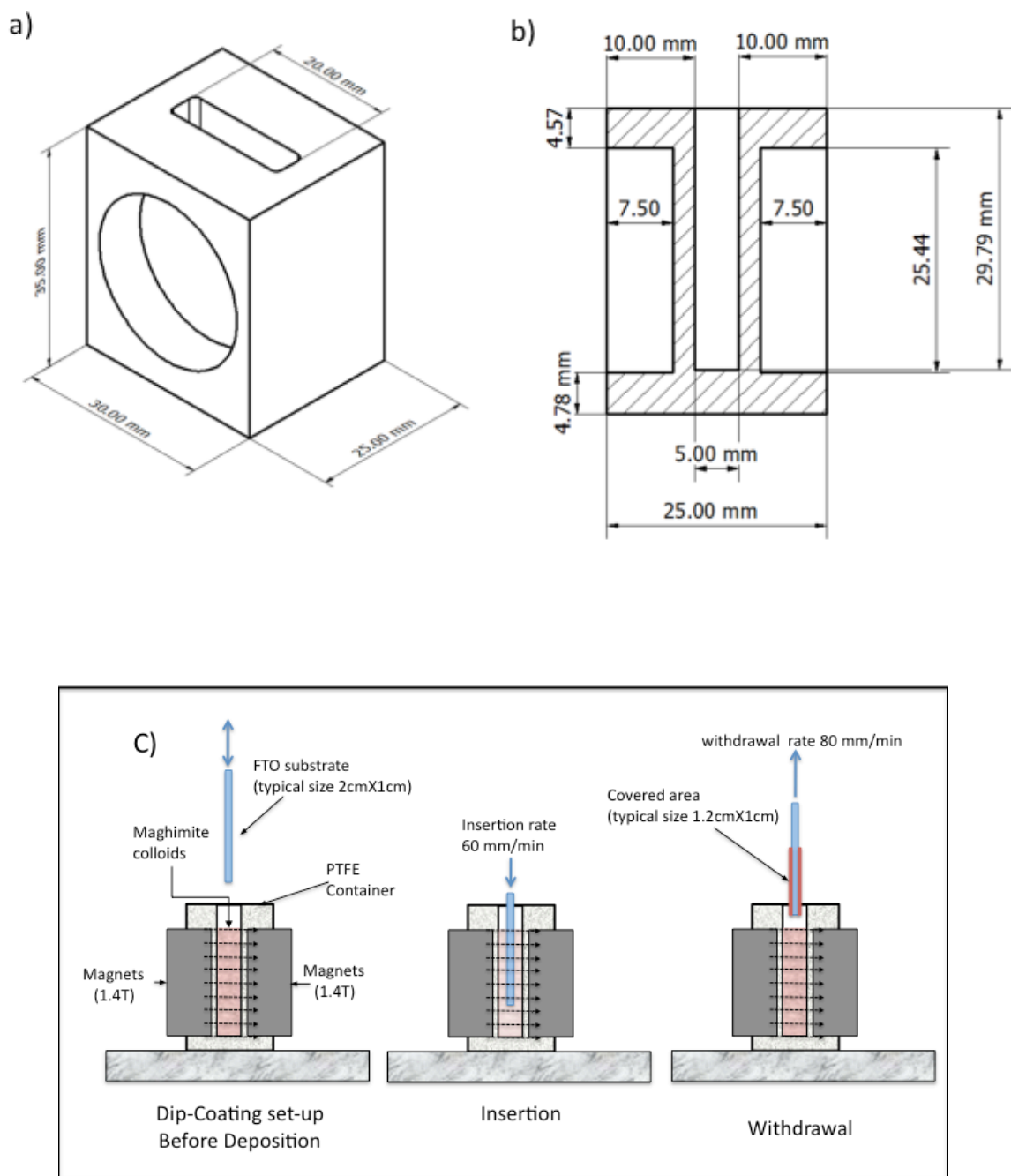


Figure S1. Dimensions of the PTFE container used in the dip-coating process with a magnetic field); a) Perspective image; b) cross-sectional image of the container with the dimensions; c) details about the dip-coating process.

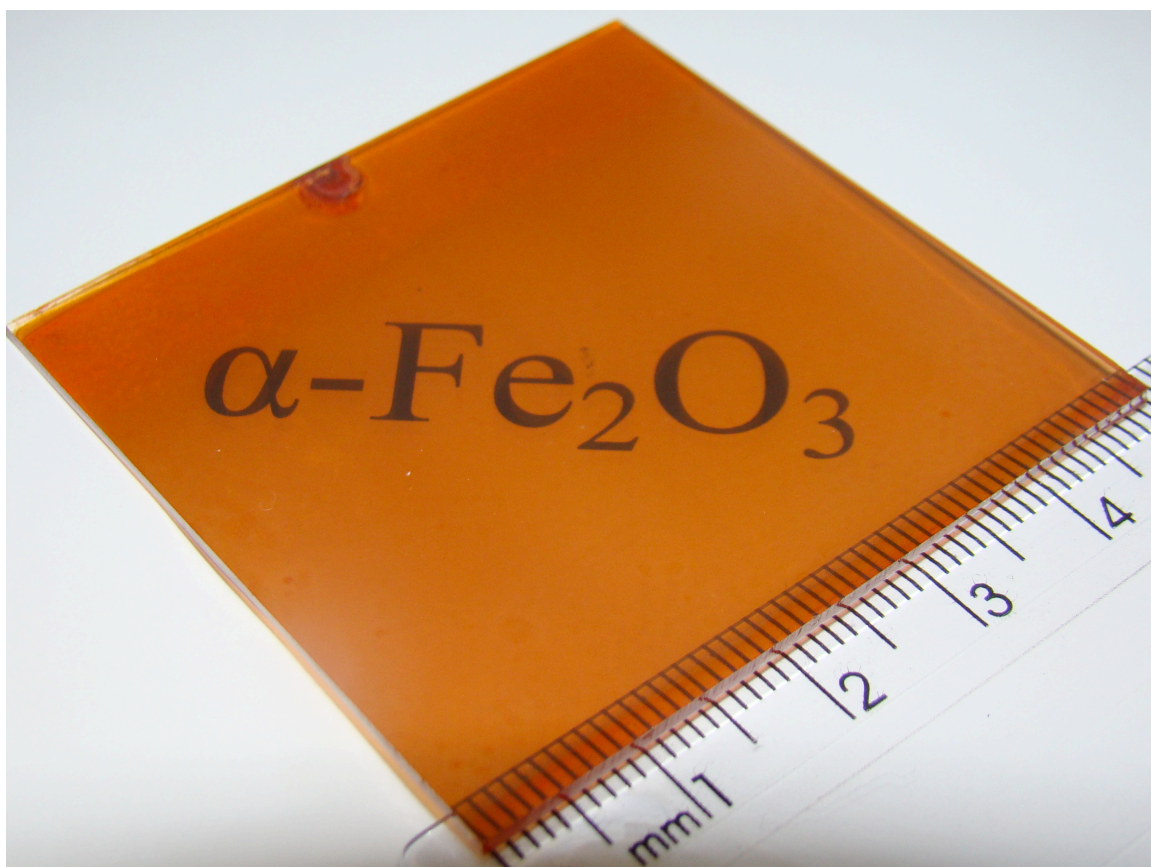


Figure S2. A hematite thin film produced by magnetic field-assisted CND on the FTO substrate with an area of 5 cm x 5 cm.

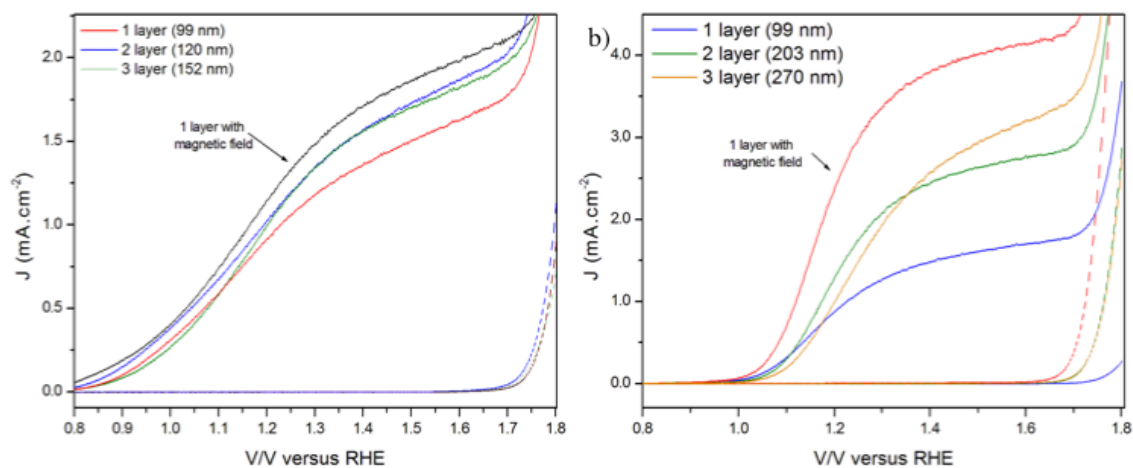


Figure S3. Comparison of the current potential curve for hematite produced with and without a magnetic field applied during the dip-coating deposition process: a) Undoped hematite; and b) Sn-doped hematite. Note that the magnetic field improves the photoelectrochemistry performance during the deposition process. Even with multiple deposition circles (without a magnetic field), photoanodes did not achieve the same performance as photoanodes processed with an external magnetic film. The undoped hematite photoanode was sintered at 850 °C for 20 minutes, and the Sn-doped hematite photoanode was sintered at 850 °C for 3 min. The film thickness is indicated in the Figure legend for the films prepared without the magnetic field.

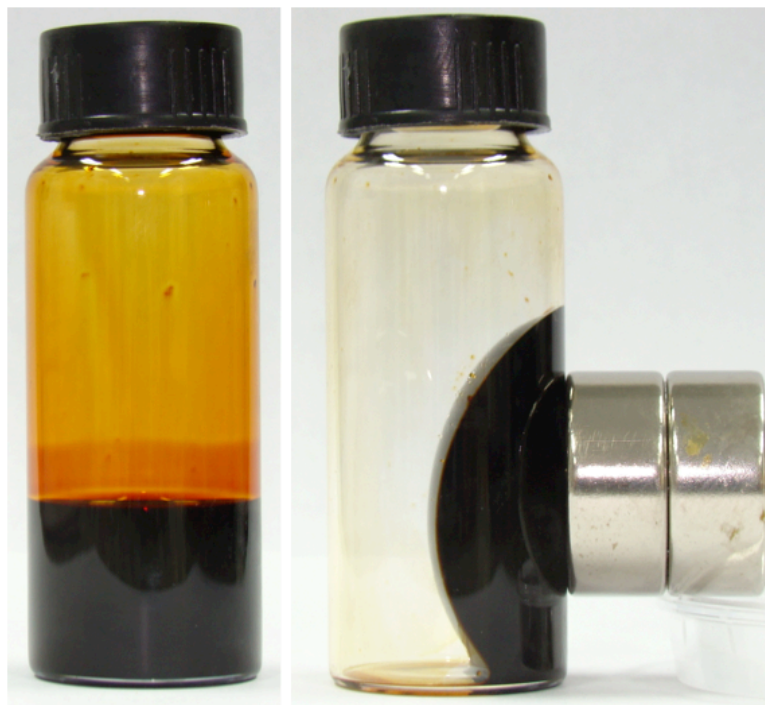


Figure S4. Photography of vessels containing maghemite colloidal dispersion without the influence of magnetic field and under the influence of an external magnetic field. We can notice that there is no phase separation between the nanoparticles and the solvent. The entire dispersion is attracted by the magnetic field. This is a typical behavior of MR fluid.

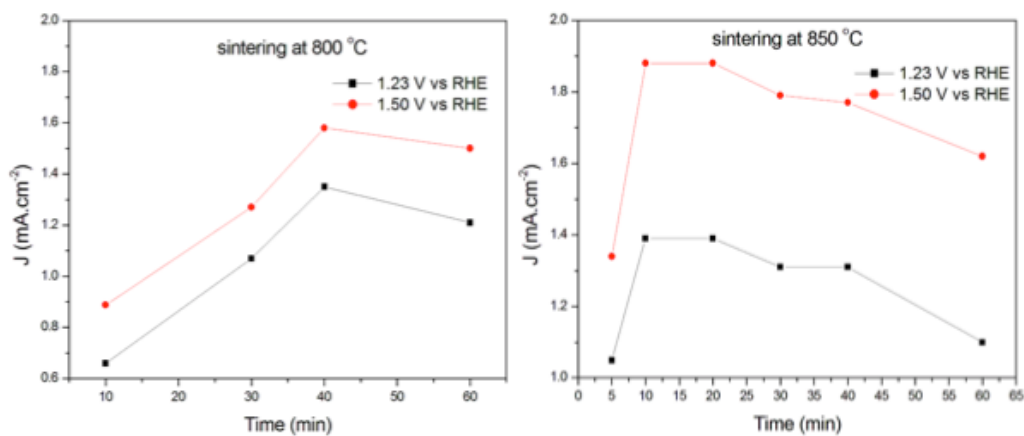


Figure S5. Current density (at 1.23 V_{RHE}) vs. sintering time for the undoped hematite thin film: a) Sintered at 800 °C; and b) Sintered at 850 °C

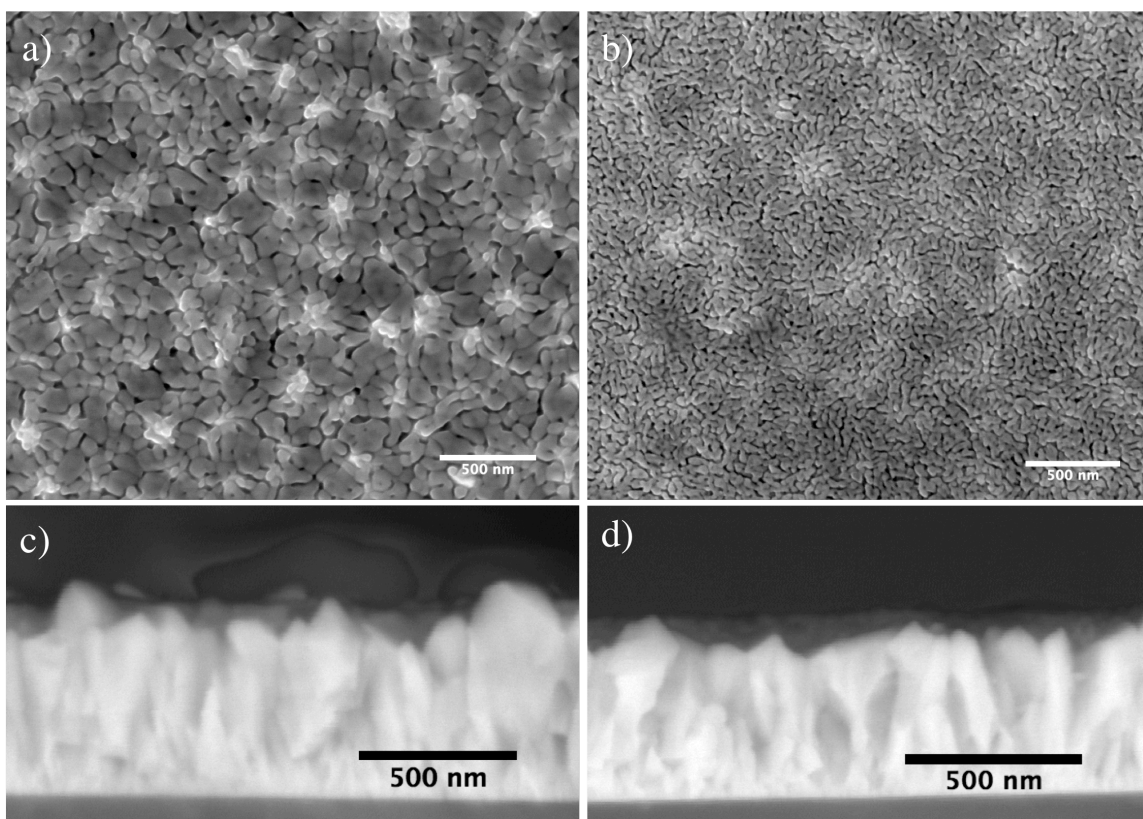


Figure S6. Comparison of SEM images of hematite thin films produced by CND without magnetic field: a) undoped hematite; and b) doped hematite.

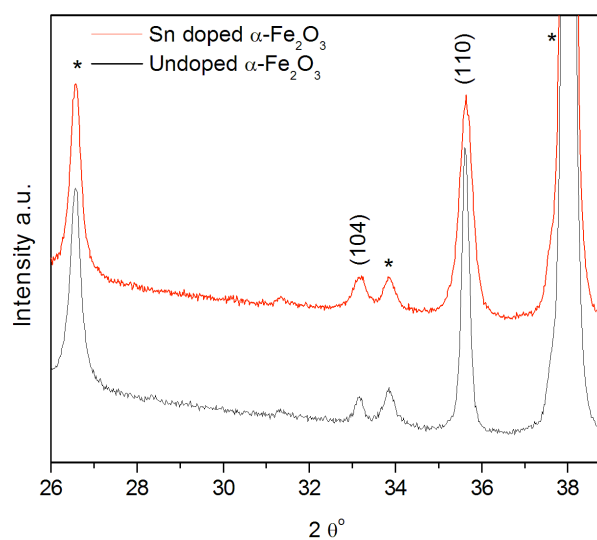


Figure S7. XRD pattern for both Sn-doped (red line) and undoped (black line) hematite thin films. * Indicates SnO_2 peak from the TCO substrate.

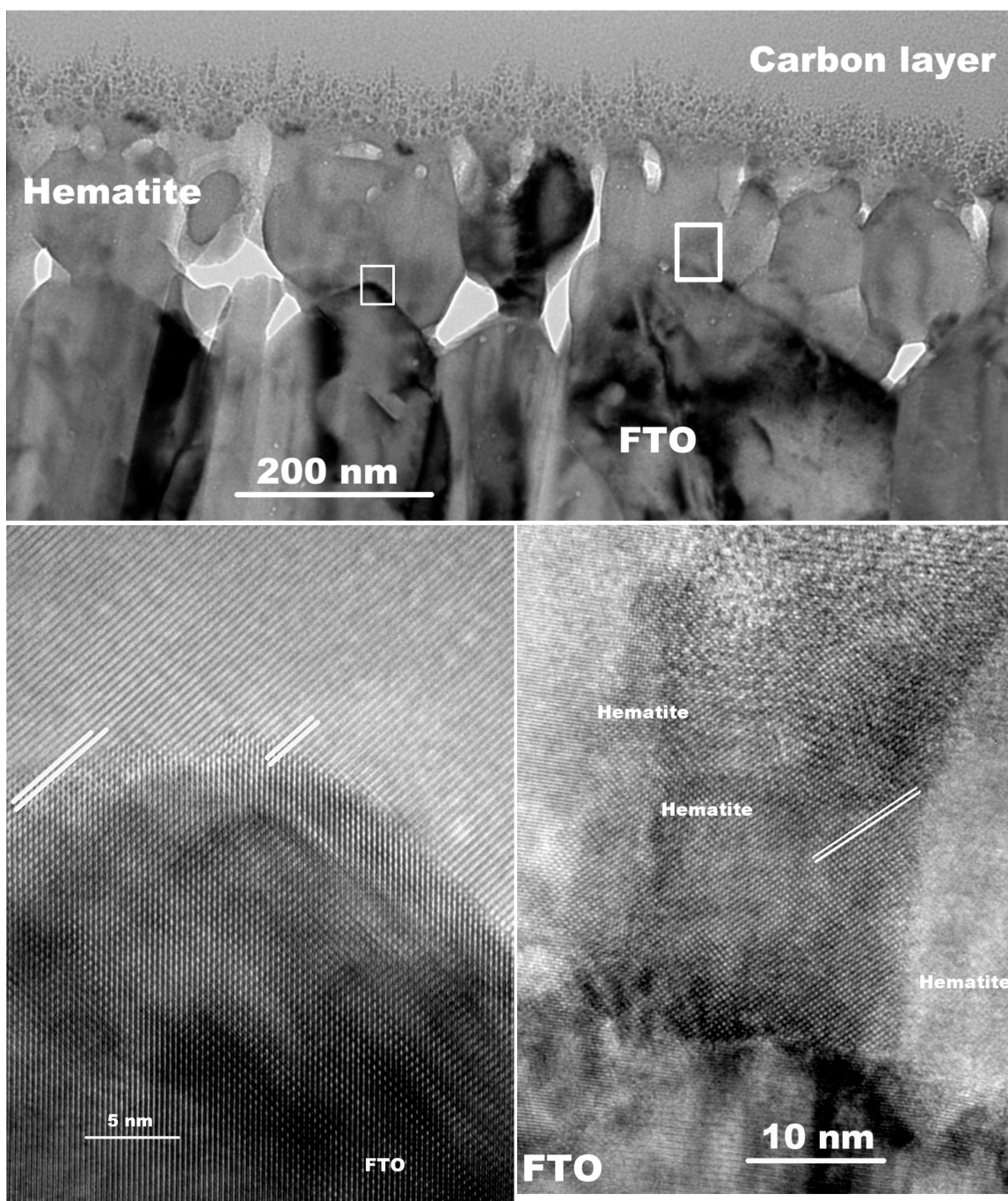


Figure S8. TEM and HRTEM cross-sectional analysis of the undoped hematite photoanode: a) Low magnification bright field TEM image showing the columnar structure; b) HRTEM image of the FTO/Hematite interface; and c) HRTEM image showing a coherent hematite grain boundary.

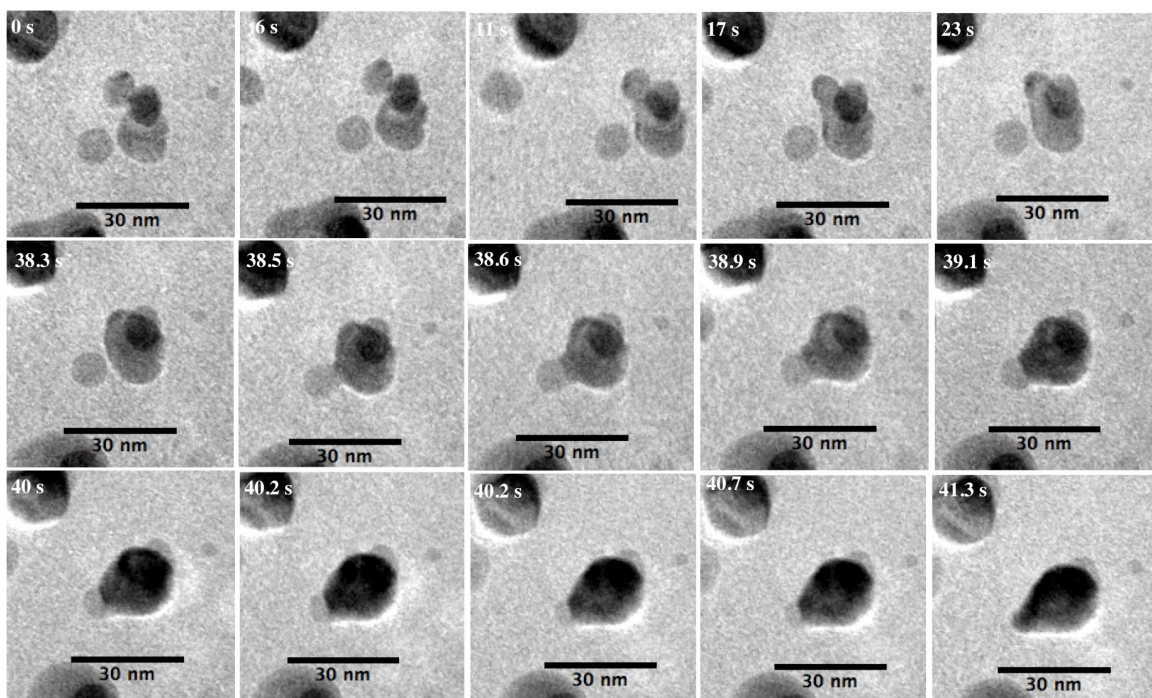


Figure S9. *In situ* bright field TEM images obtained at 850 °C showing a sequence of images as a function of the time.

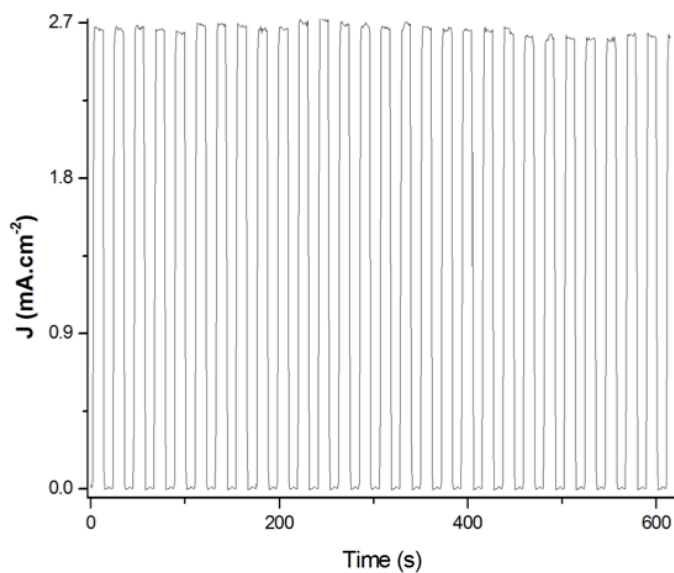


Figure S10. Chronoamperometry test, performed at 1.23 V_{RHE} which shows electrochemical stability for the Sn-doped hematite photoanode.

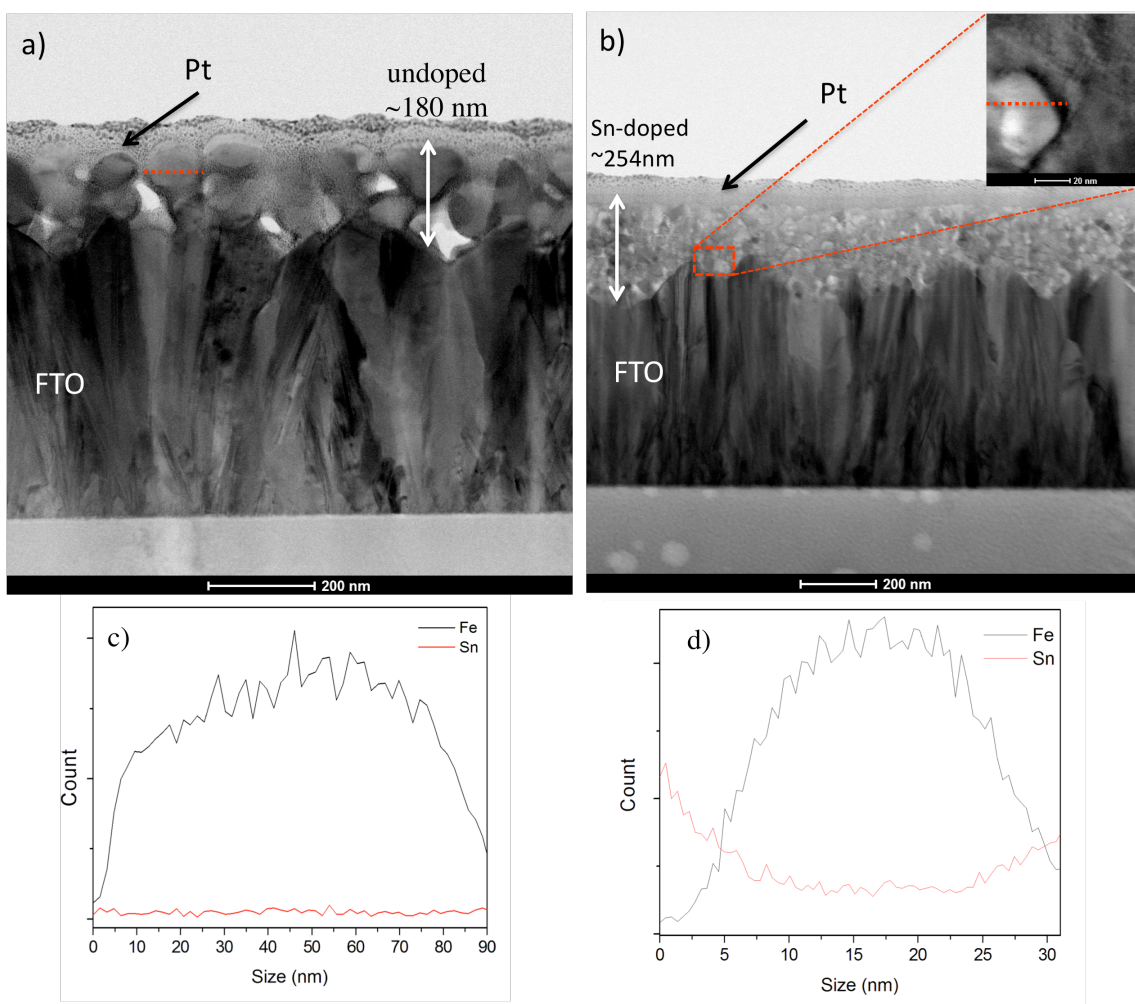


Figure S11. STEM cross-sectional image of: a) Undoped hematite with a thickness of ~180 nm.;b) STEM image of Sn-doped hematite with a thickness of ~254 nm; c) plot corresponding to the line scan (EDX) for undoped hematite (the red line in the figure (a) shows the analyzed region; and d) the EDX line scan for Sn-doped hematite (the red line in the inset shows the analyzed region) .

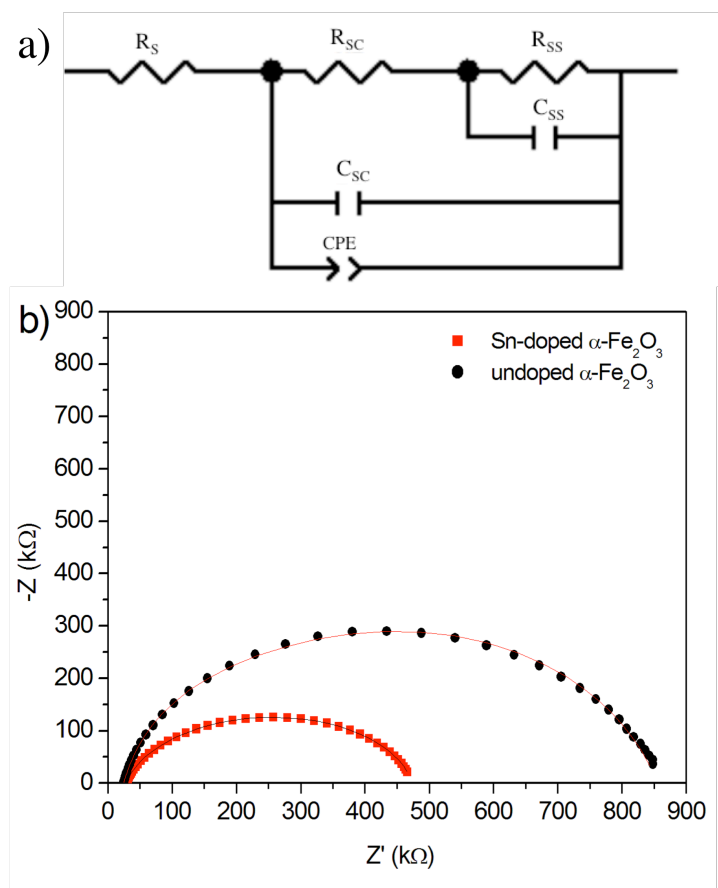


Figure S12. Measured electrochemical impedance spectroscopy for undoped and doped hematite thin films: a) The equivalent circuit diagram used to simulate and to fit the Nyquist plot of hematite photoanodes; R_s represents the ohmic serial resistance of the system; C_{ss} and R_{ss} represent surface state capacitance and surface state resistance, respectively; R_{sc} and C_{sc} correspond to the semiconductor space-charge resistance and capacitance, respectively; CPE corresponds the constant phase element associated with the Helmholtz layer; and b) Nyquist plot for both undoped and doped thin films; the continuous red line represents the fit which is based on the equivalent circuit diagram depicted in (a).

Table S1. Fitted parameters obtained from the equivalent circuit diagram used to simulate and to fit the Nyquist plot of hematite photoanodes (Figure S12)

	R_s (Ω)	R_{sc} (Ω)	R_{ss} (Ω)	C_{ss} (F)	C_{sc} (F)	$CPE1-T(s^p/\Omega)$	$CPE1-P$ (0.8-1)	q^2
Undoped	24.84	57.35	798.7	1.0776E-6	2.239E-7	2.0447E-5	0.63806	3.303E-5
Sn-Doped	28.88	24.55	448	2.4987E-7	7.3382E-7	7.2885E-5	0.56131	1.78E-4

Table S2. N_D and V_{fb} values extracted of Mott-Schottky plot for both thin thin films.

Hematite Photoanode	N_D (cm^{-3})	V_{fb} (V_{RHE})
Undoped	1.3×10^{18}	0.40
Sn-doped	1.7×10^{18}	0.94

Reference

[1] R.H. Goncalves, B. H. R. Lima, E. R. Leite, *J. Am. Chem. Soc.*, 2011, **133** (15), 6012–6019.